

Enhanced Photogalvanic Cell for Solar Energy Using Neutral Red, DTAB, and Cellobiose in Alkaline Solution

Meenakshi Jonwal* 

Department of Chemistry, Jai Narain Vyas University, Jodhpur, Rajasthan, India

*Correspondence: meenakshi.jp.04@gmail.com

ORCID: <https://orcid.org/0000-0001-6849-3567>

Received: 27th September, 2025; Accepted: 15th October, 2025; Published: 31st October, 2025

Vantage: Journal of Thematic Analysis

A Peer Reviewed Multidisciplinary Publication of Centre for Research, Maitreyi College, University of Delhi. Volume 6, Issue 2, October 2025. <https://vantagejournal.com>, ISSN(E): 2582-7391

How to cite:

Meenakshi Jonwal. (2025). Enhanced Photogalvanic Cell for Solar Energy Using Neutral Red, DTAB, and Cellobiose in Alkaline Solution. *Vantage: Journal of Thematic Analysis*, 6(2), 58-82. <https://doi.org/10.52253/vjta.2025.v06i02.58>

ABSTRACT

This study details a comprehensive investigation into the photogalvanic properties of a stable Neutral Red non-ionic dye photosensitizer system. It has been conducted in the presence of Dodecyl trimethyl Ammonium Bromide (DTAB) surfactant and cellobiose reductant within an alkaline medium, with the primary aim of advancing solar energy conversion and storage capabilities. The novelty of this research consists in the substantial improvement in electrical performance achieved compared to prior photogalvanic cell studies. The optimized system demonstrated impressive metrics, including a maximum potential of 916 mV, a maximum current of 10000 μ A, a power at power point of 847 μ W, a fill factor of 0.26, and a conversion efficiency of 10.95%. These high-performance indicators underscore the practical relevance of the study and its potential to contribute to more efficient photogalvanic technology. The achieved performance is attributed to the meticulous optimization of various cell fabrication parameters, leading to a synergistic enhancement of the system's overall efficiency and stability.

Keywords: Solar Energy, Photogalvanic Effect, Spectral Study, Dodecyl trimethyl Ammonium Bromide, Cellobiose, Neutral Red.

1. INTRODUCTION

Solar energy has emerged as a cornerstone of the global renewable energy transition, with photovoltaic (PV) technology leading the charge due to its potential for continuous efficiency improvements and declining costs (Green et al., 2022; IEA (2020); NREL, n.d.). Laboratory-scale crystalline silicon (c-Si) solar cells have achieved efficiencies exceeding 26%, while commercial modules now approach 24%, making PV competitive with conventional energy sources worldwide (IEA (2020); NREL, n.d.).

However, a critical limitation of conventional PV systems is their inability to intrinsically store the generated electricity, which necessitates costly external battery systems to ensure continuous power supply—particularly for off-grid and rural applications (Zakeri & Syri, 2015).

Photogalvanic (PG) cells are a promising alternative, that simultaneously enable solar energy conversion and storage in a single device. In a PG cell, which is based on Becquerel effect a photosensitizer absorbs incident light and initiates a redox reaction within the electrolyte, generating an electrical current while

storing energy in the chemical form (Becquerel, 1839; Hillson & Rideal, 1953; Hoffman & Lichtin, 1979; Rabinowitch, 1940b). This unique dual functionality makes PG cells particularly attractive for decentralized applications, rural electrification, and regions with intermittent sunlight. The concept of photogalvanics was pioneered by Rabinowitch (Rabinowitch, 1940a), who first described the photogalvanic effect in dye solutions and established its fundamental principles. Subsequent decades have witnessed investigations into PG mechanisms, component optimization, and performance enhancement, with significant contributions by various researchers (Albery, 1982; Ameta et al., 1985; K. M. Gangotri & Regar, 1996; Kaneko & Yamada, 1977; Koli et al., 2012; C. Lal, 2007; Murthy & Reddy, 1979; Solanki & Gangotri, 2011). These works highlighted the decisive role of photosensitizers, reductants, surfactants, and electrodes in determining PG efficiency, stability, and storage capacity.

Recent studies have focused on enhancing PG performance through innovative materials and electrolyte formulations. Investigations into mixed surfactant systems (M. Lal & Gangotri, 2025), mixed dye systems (K. M. Gangotri & Lal, 2000; Koli, 2014a; Yadav & Lal, 2013), novel reductants (Mall et al., 2022), and optimized electrode configurations (Jonwal et al., 2022; Koli & Saren, 2024), have yielded measurable improvements in charge-transfer kinetics, durability, and overall conversion efficiency. However, the efficiency and long-term stability of PG cells remain below those of mature PV technologies, requiring systematic optimization of their constituent components.

The present work explores the photogalvanic performance of a system based on Neutral Red as a non-ionic dye photosensitizer, Dodecyl Trimethyl Ammonium Bromide (DTAB) as a surfactant, and cellobiose as a reductant in an alkaline medium. Neutral Red was chosen for its favourable diffusivity, inherent stability, and good conductivity, properties that have proven beneficial in PG systems (Jonwal et al., 2025). DTAB was incorporated to improve solubility and diffusion kinetics of the redox couple, consistent with previous reports on surfactant-enhanced PG performance (Bahri et al., 2006; Jonwal et al., 2022). Cellobiose was introduced as a novel reductant, hypothesized to provide a stable and efficient redox environment.

A PG cell was fabricated with the following configuration: 0.5 ml of M/500 Neutral Red, 1.0 ml of M/10 DTAB, 1.0 ml of M/100 cellobiose, 16 ml of 1 M NaOH, 16.5 ml of water, a platinum working

electrode (0.2×0.15 cm), and a 5 cm cylindrical graphite counter electrode. The system demonstrated a substantial improvement over previous PG reports, with a maximum potential of 916 mV, a maximum current of 10,000 μ A, power at power point of 847 μ W, a fill factor of 0.26, and a solar-to-electrical conversion efficiency of 10.95%. In addition to higher efficiency, the system exhibited enhanced stability and energy storage capacity compared to earlier studies.

This work aims to systematically analyse the synergistic effects of Neutral Red, DTAB, and cellobiose, and to identify the optimum combination of cell variables for maximizing the photogalvanic performance of this novel configuration. By addressing the interdependent roles of photosensitizer, surfactant, and reductant, this study contributes toward advancing PG cells as a viable technology for integrated solar energy conversion and storage.

2. EXPERIMENTAL SECTION

2.1 Materials and Reagents

The chemicals employed in this photogalvanic investigation were procured from Loba Chemie and used without further purification. The key reagents included: M/10 Dodecyl trimethyl Ammonium Bromide (DTAB) as the surfactant, M/500 Neutral Red as the photosensitizer, M/100 Cellobiose as the reductant, and 1M Sodium hydroxide (NaOH) to establish the alkaline medium. All solutions were meticulously prepared using singly distilled water. For the electrochemical processes, platinum was selected as the working electrode, serving as the site where the primary redox reactions occur. Graphite was utilized as the counter electrode, essential for completing the electrical circuit and enabling current measurement.

Characteristics of Chemicals

A detailed understanding of the chemical characteristics is crucial for interpreting their roles in the photogalvanic system and ensuring reproducibility of the experimental findings.

Dodecyl trimethyl Ammonium Bromide (DTAB)

This compound possesses a molecular formula of $C_{15}H_{34}BrN$ and a molecular weight of 308.34 g/mol. It is characterized by its cationic nature, with an IUPAC name of Dodecyl(trimethyl)azaniumbromide. DTAB appears as a white, water-soluble, hygroscopic powder. While generally stable under normal conditions, it is incompatible with oxidizing agents due to its cationic surfactant properties. Its industrial applications include use as an antistatic agent,

preservative, and hair conditioning agent. The cationic nature of DTAB is particularly relevant in this study, as it can interact with the non-ionic Neutral Red dye and influence its solubility and diffusion within the electrolyte, thereby enhancing the overall cell performance.

Neutral Red

The photosensitizer, Neutral Red, has a molecular formula of $C_{15}H_{17}ClN_4$ and an IUPAC name of 2,8 Phenazine Diamine. Its molecular weight is 288.78 g/mol, and it exhibits a maximum absorption wavelength (λ_{max}) at 527 nm. Neutral Red is recognized for its versatility, functioning as a pH indicator, a general dye, an acid-base indicator, and a stain in histology. It is also known by synonyms such as nuclear red chloride, basic red 5, or toluylene red. The dye is highly soluble in water, with a solubility of 50 g/l at 25°C. The non-ionic nature of Neutral Red and its pH indicator properties are directly pertinent to its behavior as a photosensitizer in an alkaline medium, highlighting the importance of pH optimization for its electrochemical activity and solubility.

Cellobiose

This disaccharide, with the molecular formula $C_{12}H_{22}O_{11}$, served as the reductant in the photogalvanic cell. Its role is to donate electrons to the excited dye molecules, facilitating the regeneration cycle essential for continuous photocurrent generation.

Sodium Hydroxide (NaOH)

Commonly known as caustic soda, Sodium Hydroxide was employed as the alkaline medium. The alkalinity of the solution is a critical factor influencing the solubility and electrochemical properties of the dye and the overall cell performance.

All chemical solutions were prepared using singly distilled water (molecular formula H_2O , molecular weight 18). Stock solutions were stored in amber-colored containers to protect them from exposure to sunlight, thereby preventing photodegradation and maintaining their chemical integrity.

2.2 Instrumentation and Apparatus

The experimental setup for studying the photogalvanic cell involved several key instruments and apparatus to ensure precise measurements and controlled conditions. The central component was an H-shaped glass tube, which was externally blackened to prevent ambient light from entering, except through a small, designated illumination window. This design ensures that light interaction is confined to the illuminated chamber.

Electrical measurements were performed using a single turn 470K potentiometer for varying circuit resistance, and digital multi-meters (specifically Haoyue DT830D and HTC 830L+) for accurately measuring current and photopotential. A plug key (AIM plug key one-way brass block) served as a switch to control the circuit closure for current measurements. Light intensity, a critical experimental parameter, was quantified using a METRAVI 207 Solar Power Meter. For detailed characterization of the dye and solution, a PerkinElmer LAMBDA 850+ UV/Vis Spectrophotometer was utilized for spectrophotometry studies. The Eutech Instrument Cyberscan CON 1500 conductivity meter was employed for conductometric studies of the solutions, providing information on ionic mobility.

The electrodes consisted of a platinum working electrode, precisely sized at 0.2 cm×0.15 cm, and a five cm long cylindrical graphite counter electrode. Copper wires were used for electrical connections. The illuminating source for charging the cell was a 200-watt incandescent bulb (Surya).

2.3 Photogalvanic Cell Fabrication and Measurement Procedures

Cell Preparation and Electrolyte Composition

The fabrication of photogalvanic cells commenced with the preparation of stock solutions. Pure chemicals were accurately weighed and dissolved in singly distilled water to create solutions of the alkali, reductant, surfactant, and dye. These individual stock solutions were then mixed in various precise volumes to formulate different electrolyte compositions for the photogalvanic cells. A consistent total electrolyte volume of 35 ml was maintained across all experimental setups.

The prepared electrolyte solution, containing the dye photosensitizer, surfactant, and reductant in an alkali medium, was carefully introduced into the H-shaped glass tube. As previously noted, this tube was blackened to ensure that light penetration was restricted solely to the designated window in one of its arms, referred to as the illuminated chamber. The platinum electrode, serving as the negative terminal, was immersed in the illuminated chamber, while the graphite electrode, acting as the positive terminal, was placed in the dark chamber of the cell. Electrical connections from the platinum and graphite electrodes were established to the digital multi-meters, potentiometer, and key using connecting wires, as visually represented in Figure 1.

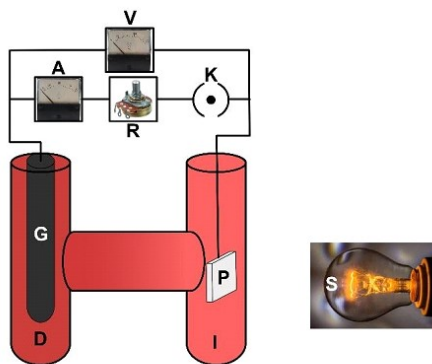


Figure 1. Photogalvanic cell apparatus (Jonwal et al., 2025) K: Key, D: Dark Chamber, G: Graphite Electrode, V: Voltmeter, I: Illuminated Chamber, S: Source, R: Potentiometer, P: Platinum Electrode, A: Ammeter

This figure provides a clear schematic of the H-shaped glass cell, illustrating the placement of the platinum working electrode in the illuminated chamber and the graphite counter electrode in the dark chamber. It also depicts the connections to the microammeter (A), digital pH meter (V), potentiometer (R), and key (K), with the light source (S) illuminating one arm. This visual representation is fundamental for understanding the physical arrangement of the experimental components, which is vital for replicating the experiment and interpreting the observed electrical responses.

Electrical Performance Measurement Protocols

The characterization of the photogalvanic cell's electrical performance followed a systematic protocol. Initially, the assembled cell, containing the electrolyte solution, was kept in complete darkness. This allowed the system to reach a stable potential value, termed the "dark potential," before any illumination was introduced. Following the dark potential measurement, the electrolyte solution was exposed to light. Upon illumination, a noticeable increase in potential was observed, rising to a peak value referred to as the "maximum potential" (V_{max}). Subsequently, the potential would stabilize at a slightly lower, consistent value known as the "open-circuit potential" (V_{oc}), under open-circuit conditions. To measure current, the circuit was subsequently closed. The resistance of the circuit was then minimized using the potentiometer to obtain the "maximum current" (i_{max}). After a brief period, the current would stabilize at a value typically less than i_{max} , which is designated as the "short-circuit current" (i_{sc}).

To comprehensively understand the cell's behavior under varying electrical loads, the resistance of the circuit was systematically increased. This process caused the current to gradually decrease from i_{sc} down to zero. At each step, the corresponding potential value was recorded, allowing for the generation of the current-voltage (i-V) characteristics curve. From these i-V pairs, the corresponding power (calculated as the product of current and potential, $i \times v$) was determined. The highest product of the current and its corresponding potential obtained from the i-V characteristics study was defined as the "power at power point" (PPP). The specific current and potential values at this peak power point were denoted as i_{pp} and V_{pp} , respectively.

Calculation of Performance Parameters

The overall performance of the photogalvanic cell was rigorously analyzed using several key electrical parameters:

- Maximum photo-potential
- Maximum photocurrent
- Short-circuit current
- Power at power point
- Fill factor (FF)
- Conversion efficiency (CE)
- Storage capacity

The Fill Factor (FF), a measure of the squareness of the i-V curve and an indicator of cell quality, was calculated using the formula:

$$FF = (V_{pp} \times i_{pp}) / (V_{oc} \times i_{sc})$$

The Conversion Efficiency (CE), representing the effectiveness of the cell in converting light energy into electrical energy, was calculated as:

$$CE = (V_{pp} \times i_{pp} \times FF \times 100) / (I \times A)$$

Where 'I' represents the illumination intensity in mW/cm , and 'A' is the area of the platinum electrode. The product

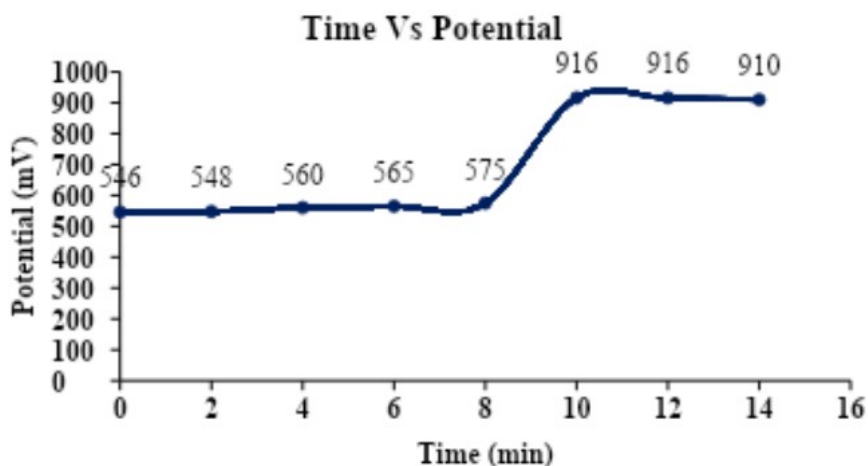
$(V_{pp} \times i_{pp})$ is expressed in mW.

The Storage Capacity of the cell was quantitatively assessed by determining the "half-change time" ($t_{0.5}$). This metric represents the duration over which the extracted power value from the cell, under dark conditions at a characteristic external load, decreases to half of its initial maximum power. The detailed definition and calculation of these electrical parameters highlight the rigorous quantitative approach employed in this study, emphasizing a

Table 1: Temporal variation of Potential

Time (min.) #	0	2	4	6	8	10	12	14*
Potential (mV)	546	548	560	565	575	916	916**	910***

[Cellobiose] 0.29×10^{-3} M, [Neutral Red Dye] 0.30×10^{-3} M, [DTAB] 2.86×10^{-3} M, Electrode Area $0.2 \text{ cm} \times 0.15 \text{ cm}$, Light Intensity 30 mW cm^{-2} , Diffusion Length 5 cm *charging time, ** V_{max} , *** V_{oc}

**Figure2 :** Temporal variation of Potential

[Cellobiose] 0.29×10^{-3} M, [Neutral Red Dye] 0.30×10^{-4} M, [DTAB] 2.86×10^{-3} M, [NaOH] 0.46 M, Electrode Area $0.2 \text{ cm} \times 0.15 \text{ cm}$, Light Intensity 30 mW cm^{-2} , Diffusion Length 5 cm

focus on overall cell performance and practical applicability beyond just peak power.

3. RESULTS AND DISCUSSION

The overall performance of the photogalvanic cells, specifically those containing DTAB surfactant, Neutral Red dye photosensitizer, and Cellobiose as a reductant, was systematically investigated across 34 different configurations. This extensive study aimed to identify and achieve the optimum cell performance by varying key fabrication parameters.

3.1 Dynamic Electrical Performance under Illumination

Potential Variation with Illumination Time

A representative photogalvanic cell was prepared with specific fabrication variables to observe its dynamic response to illumination. The composition included 1 ml of M/10 DTAB surfactant, 0.5 ml of M/500 Neutral Red dye photosensitizer, 1 ml of M/100 Cellobiose, 16 ml of 1M NaOH, and 16.5 ml of water. The electrodes used were a platinum

working electrode ($0.2 \text{ cm} \times 0.15 \text{ cm}$) and a five cm long cylindrical graphite counter electrode.

Initially, the cell exhibited a stable dark potential of 546 mV. Upon illumination, the potential rapidly increased, reaching a maximum value (V_{max}) of 916 mV within 10 minutes.¹ Following this peak, the potential stabilized at 910 mV, which is referred to as the open-circuit potential (V_{oc}), with the circuit remaining open and the load disconnected. The transient behavior of the potential during this charging phase is summarized in Table 1 and visually depicted in Figure 2. The rapid increase to V_{max} and subsequent stabilization at V_{oc} with only a small difference (916 mV vs. 910 mV) indicates efficient charge separation and the swift establishment of a stable photo potential. This behavior suggests good stability of the photo-generated species even under open-circuit conditions, which is a desirable characteristic for energy conversion devices.

Figure 2 visually represents the data from Table 1, clearly illustrating the initial dark potential, the subsequent rapid rise in potential upon illumination,

Table 2: Change of potential with current and power with current of illuminated cell

Current (μA)	Potential (mV)	Power (μW)	Current (μA)	Potential (mV)	Power (μW) [#]
8000	31	248	1400	605	847*
7000	56	392	1200	608	730
6000	78	468	1000	618	618
5000	103	515	800	630	504
4000	136	544	600	643	386
3000	210	630	400	701	280
2000	350	700	200	767	153
1800	412	742	0	801	0
1600	501	802	-	-	-

[#][Cellobiose] 0.29×10^{-3} M, [Neutral Red Dye] 0.30×10^{-4} M, [DTAB] 2.86×10^{-3} M, [NaOH] 0.46 M, Electrode Area $0.2 \text{ cm} \times 0.15 \text{ cm}$, Light Intensity 30 mW cm^{-2} , Diffusion Length 5 cm

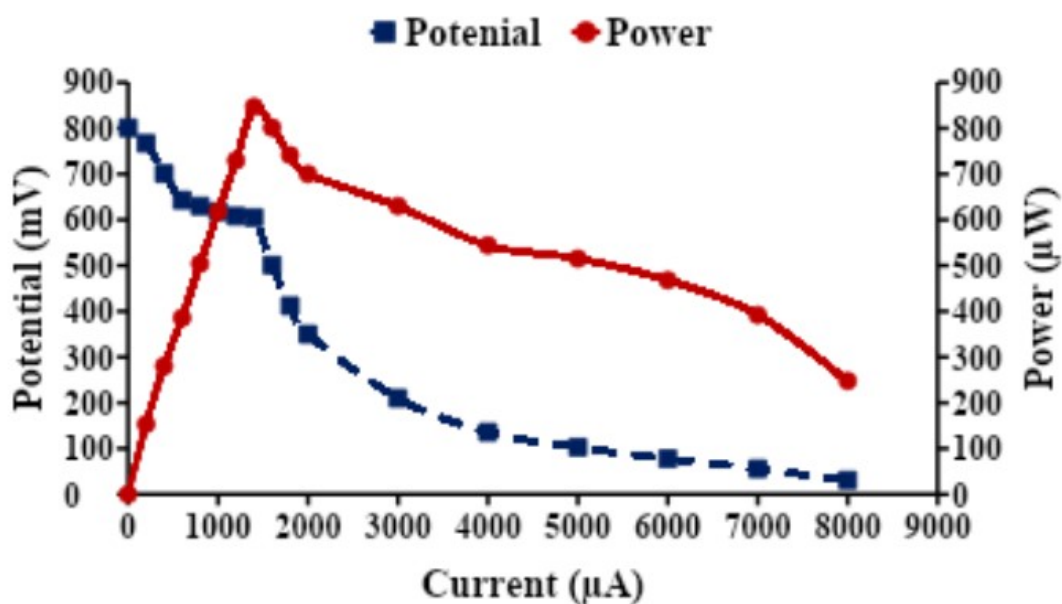


Figure 3: Change of potential with current and power with current of illuminated cell [#]. [#][Cellobiose] 0.29×10^{-3} M, [Neutral Red Dye] 0.30×10^{-4} M, [DTAB] 2.86×10^{-3} M, [NaOH] 0.46 M, Electrode Area $0.2 \text{ cm} \times 0.15 \text{ cm}$, Light Intensity 30 mW cm^{-2} , Diffusion Length 5 cm

and its eventual stabilization at the open-circuit potential. The visual trend confirms the quantitative data, making the dynamic response of the cell to light immediately apparent and easy to interpret.

Current-Voltage (I-V) Characteristics and Power Output

The I-V characteristics study revealed a consistent inverse relationship between current and potential across all tested cells. This is typical for power-generating devices, where increasing the load (and

Table 3: Cell storage capacity under dark conditions

Time (min)	Current (μA)	Potential (mV)	Power (μV)
0	1530	340	520
10	1530	310	474
20	1500	290	435
30	1480	278	411
40	1460	260	380
50	1420	255	362
60	1400	234	328
70	1360	212	288
80	1320	198	261
90	1250	167	209

#[Cellobiose] 0.29×10^{-3} M, [Neutral Red Dye] 0.30×10^{-4} M, [DTAB] 2.86×10^{-3} M, [NaOH] 0.46 M, Electrode Area $0.2 \text{ cm} \times 0.15 \text{ cm}$, Light Intensity 30 mW cm^{-2} , Diffusion Length 5 cm

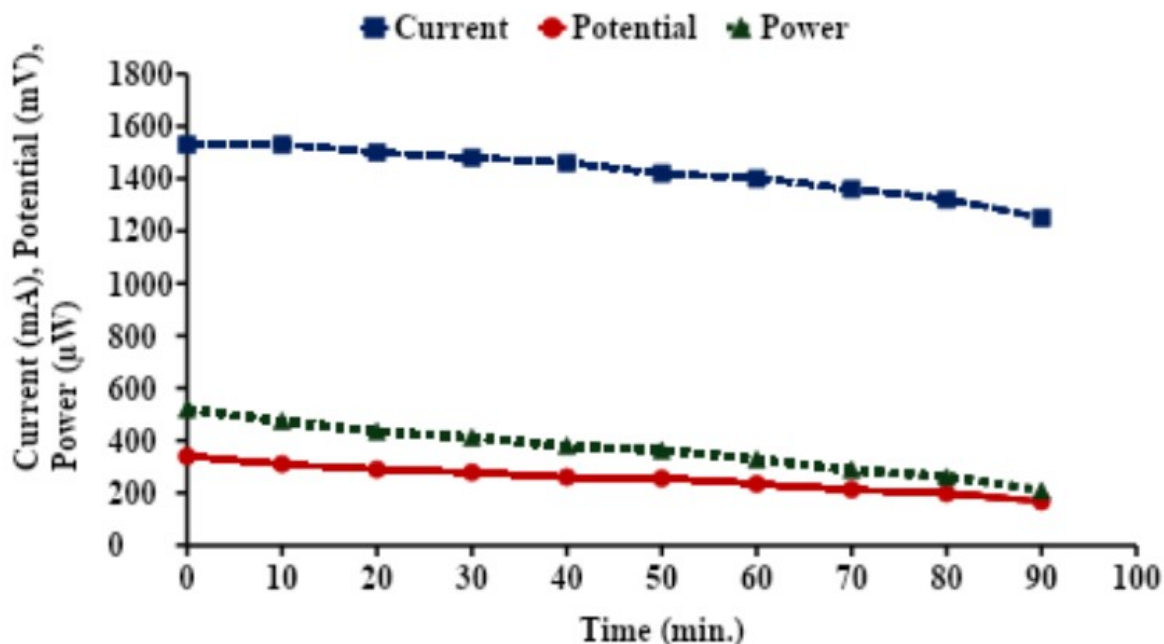


Figure 4: Cell storage capacity under dark conditions # [Cellobiose] 0.29×10^{-3} M, [Neutral Red Dye] 0.30×10^{-4} M, [DTAB] 2.86×10^{-3} M, [NaOH] 0.46 M, Electrode Area $0.2 \text{ cm} \times 0.15 \text{ cm}$, Light Intensity 30 mW cm^{-2} , Diffusion Length 5 cm

thus potential) generally leads to a decrease in current. Upon closing the circuit key, the photogalvanic cell initiated current and power generation while simultaneously undergoing charging under illuminated conditions. As the

external resistance in the circuit was progressively increased, the current output of the cell began to decrease, while the corresponding potential across the cell terminals increased.

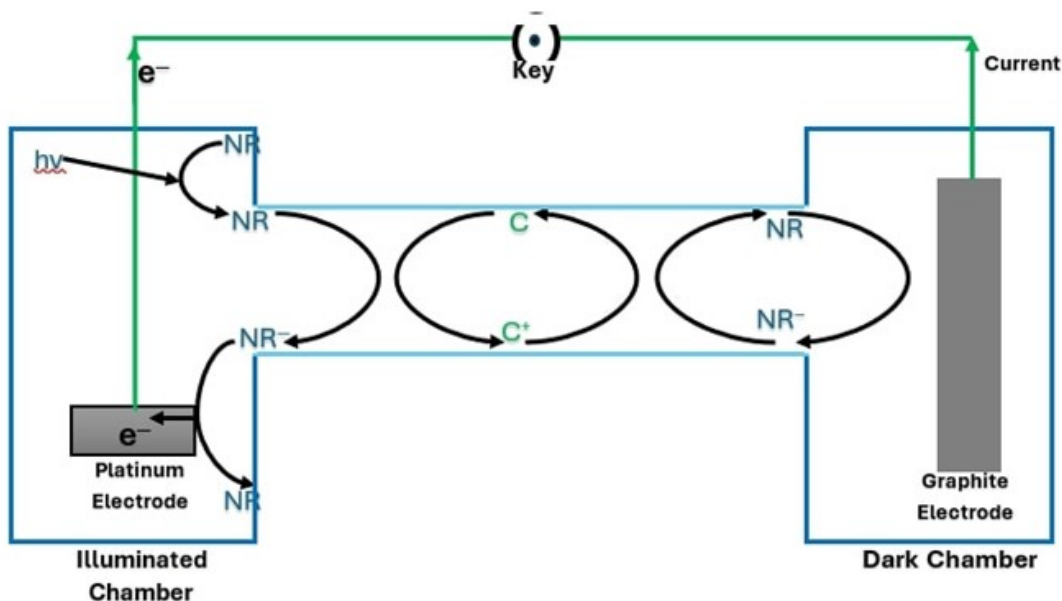


Figure 5: The mechanistic aspect of the photo-generation of the current

The maximum power extractable from the cell, known as the Power at Power Point (P_{pp}), was determined to be $844 \mu\text{W}$. This optimal power output was achieved at a current (i_{pp}) of $1400 \mu\text{A}$ and a potential (V_{pp}) of 603mV . The detailed quantitative relationship between current, potential, and power under varying load conditions is presented in Table 2 and graphically illustrated in Figure 3. The clear presence of a maximum power point indicates that the cell can be effectively optimized for power extraction under specific load conditions. The shape of the i - V curve is diagnostic for photovoltaic devices, providing crucial information about internal resistance, charge recombination, and the overall quality of the cell, thereby enabling a comprehensive performance analysis.

This figure presents the i - V curve and the power curve as a function of current, clearly illustrating the inverse relationship between current and potential. The peak in the power curve precisely indicates the maximum power point, which is the optimal operating condition for extracting the highest electrical power from the cell. The shape of this curve provides valuable information about the cell's internal losses and the efficiency of charge separation and transport, making it an indispensable diagnostic tool for evaluating photovoltaic performance.

3.2 Energy Storage and Performance in Dark Conditions

Analysis of Dark Performance

The photogalvanic cell's performance was also rigorously evaluated in the absence of light, where its function transitioned solely to that of an energy storage device, as it is inherently unable to generate power without illumination. To assess its storage capabilities, a cell fabricated with optimal variables for high electrical performance was initially illuminated for 14 minutes, serving as its charging period. Subsequently, its electrical performance was monitored in the dark under a characteristic external load (403.712).

Over time in dark conditions, a consistent decrease in the measured current, potential, and calculated power of the photogalvanic cell was observed. This decay profile is quantitatively presented in Table 3 and visually confirmed in Figure 4. A key metric for storage capacity, the "half-change time" ($t_{0.5}$), was determined to be 90 minutes. This signifies the duration required for the extracted power value to diminish to half of its initial maximum value in the dark. The 90-minute half-change time suggests a relatively stable storage capability for this photogalvanic cell, which is a notable advantage, particularly when compared to conventional batteries that store charge primarily through deposition on electrodes. This observation points towards a

fundamentally different energy storage mechanism within the photogalvanic system.

This graph visually demonstrates the discharge characteristics of the photogalvanic cell in the dark. The decreasing trends of current, potential, and power over time clearly illustrate the cell's energy retention and release capabilities. This visual evidence is as crucial as the power generation characteristics for a device designed for both solar energy conversion and storage.

Mechanism of Energy Storage

The generation of photocurrent within the photogalvanic cell inherently implies the storage of energy. However, this energy storage mechanism fundamentally differs from that of conventional batteries. In traditional batteries, energy is stored primarily through the deposition of charge on the electrodes. In contrast, within this photogalvanic system, energy is stored in the form of specific dye molecule species, particularly the leuco-form of the dye.

The process begins when light interacts with a dye molecule, causing an electron to transition from its highest occupied molecular orbital (HOMO) to a higher energy orbital, the lowest unoccupied molecular orbital (LUMO). This excitation generates two possible excited states: a triplet state or a singlet state. The triplet excited state involves a spin transition and is generally less probable, whereas the higher probability of the singlet excited state is significant because it leads to the formation of the leuco-form of the dye after reduction. It is this leuco-form that serves as the primary energy storage medium.

The observed charging and discharging cycles of the fabricated cells provide compelling evidence for the reversibility of the electrochemical phenomenon in this specific photogalvanic system, which utilizes Neutral Red as the photosensitizer, Cellobiose as the reductant, and Dodecyl trimethyl Ammonium Bromide (DTAB) as the surfactant in an aqueous Sodium Hydroxide solution.

Despite this reversibility, various factors can impede the electrical performance of the photogalvanic cell. These include the inherent decay of the dye molecules and, notably, the detrimental effect of atmospheric oxygen on the excited states of the dye molecules.¹ Since the experimental system was open to the atmosphere, atmospheric oxygen could readily quench the excited dye molecules, thereby reducing efficiency. Furthermore, an increase in the cell's temperature during the discharging process, often caused by internal resistance and the viscosity of the

solution, can lead to enhanced diffusion of atmospheric oxygen into the electrolyte. This increased oxygen diffusion further exacerbates the deterioration of the photogalvanic cell's performance.

3.3 Proposed Mechanistic Pathway for Photocurrent Generation

To gain a deeper understanding of the processes governing photocurrent generation, the photogalvanic cell, comprising DTAB surfactant, Neutral Red dye photosensitizer, Cellobiose reductant, and NaOH alkali in an aqueous medium, was investigated in detail by referencing established literature. The opto-electrochemical properties of each individual chemical constituent within the electrolyte were also meticulously studied. This approach aimed to verify and confirm the precise nature of the electroactive species and the charge carriers involved in the photogalvanic cell's operation.

Electroactive Species and Electron Transfer

Initial investigations into the opto-electrical properties of an aqueous cellobiose solution revealed a potential of 136 mV but no discernible current under dark conditions. Crucially, illuminating this aqueous cellobiose solution did not induce any change in either current or potential compared to its dark values. This observation strongly suggests that the cellobiose molecule itself is not an electroactive species; rather, it functions primarily as an electron carrier within the system.

In contrast, when the Neutral Red sensitizer was illuminated in the presence of cellobiose reductant and an alkali medium, significant changes in both current and potential were observed. This directly demonstrated the electroactive nature of the sensitizer molecules. From these comparative observations, it is definitively deduced that the Neutral Red molecule is the primary electroactive species, while the cellobiose molecule, in both its molecular and oxidized states, serves solely to facilitate electron transfer.

The proposed mechanism posits that the excited state of Neutral Red undergoes reduction to form a leuco or semi-species, which is an electroactive species, at the illuminated electrode. Concurrently, the Neutral Red molecule is inferred to act as an electroactive species at the dark electrode. This understanding is further corroborated by published literature, which indicates that both the reduced dye molecule and the dye molecule itself can function as electroactive species in photogalvanic cells.

The detailed electrochemical processes occurring during the photo-generation of current can be visualized through a flow diagram (Figure 5) and further explained by energy levels (Figure 6). The distinction between Neutral Red as the electroactive species and Cellobiose as the electron carrier is a fundamental aspect of the mechanism. This implies that the cell's efficiency is heavily reliant on the dye's ability to undergo reversible redox reactions and the stability of its excited state.

This diagram provides a visual flow of the electrochemical processes within the photogalvanic cell. It illustrates how Neutral Red (NR) absorbs a photon ($h\nu$) in the illuminated chamber to become an excited state (NR^*). This excited state then interacts with Cellobiose (C) to form a leuco or semi-reduced form (NR^-), simultaneously oxidizing Cellobiose to C^+ . The NR^- then releases an electron to the Platinum electrode, generating current. In the dark chamber, NR accepts an electron from the Graphite electrode to form NR^- , which subsequently reduces C^+ back to C, completing the cycle. This figure is essential for a clear understanding of the proposed mechanism, translating complex chemical reactions and electron flows into an easily digestible visual format.

The mechanistic pathway involves distinct processes in both the illuminated and dark chambers of the cell:

Photo-process in the illuminated chamber:

- A photon ($h\nu$) is absorbed by a Neutral Red dye molecule (NR), exciting it to its singlet excited state (NR^*).
- The excited singlet state undergoes inter-state crossing (ISC) to form the triplet excited state ($\text{NR}\{\text{T}\}$) in the bulk electrolyte.
- The triplet excited state of Neutral Red ($\text{NR}\{\text{T}\}$) is then reduced by the Cellobiose reductant (C) to form the leuco or semi-reduced form of the dye (NR (leuco or semi)), while Cellobiose is oxidized to C^+ in the bulk electrolyte.
- The leuco-form of Neutral Red (NR (leuco)) then transfers an electron (e^-) to the platinum electrode.

Photo-processes in the dark chamber:

- Neutral Red molecules (NR) in the dark chamber accept an electron (e^-) from the graphite electrode to form the semi-reduced dye form (NR^-).
- This semi-reduced dye (NR^-) then reacts with the

oxidized Cellobiose (C^+), which has diffused from the illuminated chamber into the electrolyte region near the dark chamber, to regenerate the leuco-form of Neutral Red (NR (leuco)).

- The leuco-form of Neutral Red (NR (leuco)) then reacts with Cellobiose (C) in the bulk electrolyte to complete the regeneration cycle.

In this flow diagram, NR denotes the Neutral Red dye molecule, NR^* represents the photo-excited dye molecule, NR^- signifies the semi/or leuco form of the dye molecule, C is the Cellobiose molecule, C^+ is the oxidized form of the Cellobiose molecule, and e^- represents an electron. ISC refers to the inter-state crossing process, while 'T' and 'S' denote the triplet and singlet excited states of the Neutral Red dye molecule (photosensitizer), respectively.

This figure provides a deeper, quantum-mechanical perspective on the electron transfer process, linking the observed macroscopic electrical performance to the molecular energy levels of the dye and reductant. It illustrates how light energy facilitates electron transitions and subsequent redox reactions that drive the current generation.

The electron transfer mechanism at a molecular level begins when an electron residing in the highest occupied molecular orbital (HOMO) of the Neutral Red dye molecule absorbs energy from an incoming photon. This energy absorption causes the electron to jump to a higher energy orbital, specifically the lowest unoccupied molecular orbital (LUMO), thereby forming the excited state of the dye molecule. Following this excitation, the dye molecule undergoes a reduction process. It receives an electron from the reductant, Cellobiose, into its HOMO, and subsequently loses an excess electron from its LUMO to the platinum electrode, as depicted in Figure 6.

In the dark chamber, Neutral Red dye molecules play a crucial role in completing the circuit. Due to a difference in electroactivity, these molecules readily accept an electron from the graphite electrode, forming the semi-reduced dye form. This semi-reduced dye, in turn, acts as a reducing agent, regenerating the oxidized Cellobiose molecule (C^+) that has diffused into the electrolyte region adjacent to the dark chamber. This continuous cycle of electron transfer and species regeneration is fundamental to the sustained operation of the photogalvanic cell. The detailed electron transfer pathway, encompassing HOMO-LUMO transitions, reduction by the reductant, and electron transfer to the electrodes, provides a molecular-level

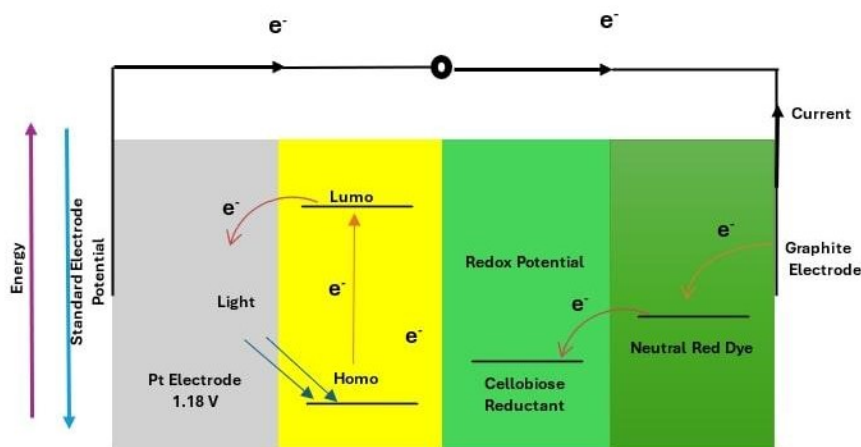


Figure 6: Photogeneration of the current in a photo-galvanic cell in terms of the standard reduction potential and energy levels

understanding of the energy conversion process, underscoring the importance of optimizing the molecular properties of the components.

4. OPTIMIZATION OF CELL FABRICATION PARAMETERS

The performance of a photogalvanic (PG) cell is highly dependent on the precise values of its fabrication variables. Achieving optimal cell performance necessitates a meticulous approach to identifying the most effective concentrations of chemical components and physical parameters. The main components influencing cell performance include the nature and concentrations of the sensitizer, reductant, surfactant, alkali, and solvent, as well as the electrode material, electrode size, diffusion length, illumination intensity, and illumination window size.

To systematically determine the optimal value for each variable, the experimental methodology involved fabricating multiple cells where only one specific variable was altered, while all other parameters were kept constant. In the current study, the PG cells were based on Neutral Red dye as the photosensitizer, DTAB as the surfactant, Cellobiose as the reductant, and NaOH as the alkali in an aqueous medium, utilizing a platinum working electrode, a graphite counter electrode, and an H-shaped glass tube. The optimization of these variables was guided by findings from previously published studies.

The comprehensive optimization process involved varying the concentrations of the alkali, dye, surfactant, and reductant, in addition to adjusting

physical factors such as platinum electrode size, illumination intensity, and illumination window size. This systematic variation resulted in the fabrication and testing of a total of 34 distinct PG cell configurations. The performance of each cell during optimization was rigorously assessed using a suite of electrical parameters, including maximum current (i_{max}), short-circuit current (i_{sc}), current at power point (i_{pp}), open circuit potential (V_{oc}), potential at power point (V_{pp}), conversion efficiency (C.E.), fill factor (FF), and charging time. This systematic variation of multiple parameters across numerous cells demonstrates a robust experimental design, crucial for identifying true optimal conditions and understanding the complex inter-dependencies within the photogalvanic system.

4.1 Influence of Alkali (NaOH) Concentration

The concentration of sodium hydroxide (NaOH) serving as the alkaline medium was identified as a critical factor influencing cell performance. To investigate this effect, five distinct cells were fabricated, each containing a different concentration of NaOH, while maintaining constant concentrations of all other chemical components and physical parameters such as diffusion length, electrode area, and light intensity. Each cell was charged under a consistent illumination intensity of 30 mWcm^{-2} .

While the general patterns of potential change with time during charging (Figure 2), i-V characteristics (Figure 3), and performance decay in dark conditions (Figure 4) remained consistent across these cells, the specific quantitative values for charging time, current, power, and potential varied significantly

Table 4: Chemical composition of cells produced for alkali concentration optimization

Cell S.N.	Volume of solutions of chemicals used to prepare 35 ml electrolyte mixture [#]					Resultant concentrations			
	1M NaOH (ml)	M/500 Neutral Red (ml)	M/100 Cellobiose (ml)	M/10 DTAB (ml)	Distilled Water (ml)	NaOH M	Neutral Red $\times 10^{-4}$ M	Cellobiose $\times 10^{-3}$ M	DTAB $\times 10^{-3}$ M
1.	14	0.5	1.0	1.0	18.5	0.40	0.30	0.29	2.86
2.	15	0.5	1.0	1.0	17.5	0.43	0.30	0.29	2.86
3.	16	0.5	1.0	1.0	16.5	0.46	0.30	0.29	2.86
4.	17	0.5	1.0	1.0	15.5	0.48	0.30	0.29	2.86
5.	18	0.5	1.0	1.0	14.5	0.51	0.30	0.29	2.86

[#]Pt Electrode Area 0.2 cm \times 0.15 cm, cylindrical graphite counter electrode, Light Intensity 30 mW cm⁻², Diffusion Length 5 cm

Table 5: Electrical parameters of the five different cells fabricated by variation of alkali concentration

Electrical parameters	[NaOH] [#]				
	0.40 M	0.43 M	0.46 M	0.48 M	0.51 M
V _{dark} (mv)	487	498	546	490	475
V _{max} (mv)	855	879	916	897	883
V _{OC} (mv)	850	876	910	890	880
t _{charging} (min.)	18	18	16	17	20
i _{max} (μ A)	5000	6000	10000	5000	4000
i _{SC} (μ A)	3500	5000	8000	6000	5500
P _{pp} (μ W)	345	505	847	621	466
V _{PP}	345	421	605	444	388
i _{PP}	1000	1200	1400	1400	1200
C.E. (%)	4.45	6.47	10.95	8.04	4.98
F.F.	0.12	0.12	0.12	0.12	0.10

[#]At [Cellobiose]0.29 $\times 10^{-3}$ M, [Neutral Red Dye]0.30 $\times 10^{-4}$ M, [DTAB]2.86 $\times 10^{-3}$ M, Electrode Area 0.2 cm \times 0.15 cm, Light Intensity 30 mW cm⁻², Diffusion Length 5 cm

between different alkali concentrations. The chemical compositions of the cells specifically fabricated for this alkali optimization are detailed in Table 4, and their corresponding electrical parameters are presented in Table 5.

The electrical performance data clearly indicates that the power output of the cell initially increases with an increase in NaOH concentration in the electrolyte solution. This power reached its maximum value at an optimal alkali concentration of 0.46 M. Beyond

this concentration, the cell power began to decrease. This observed trend is consistent with prior studies, which have also reported that cell performance improves with increasing alkalinity up to an optimal concentration.¹

The explanation for this behavior lies in the chemical properties of the system. As the concentration of NaOH increases, the alkalinity and consequently the pH of the solution also rise. This increase in pH plays a crucial role in enhancing the solubility of Neutral

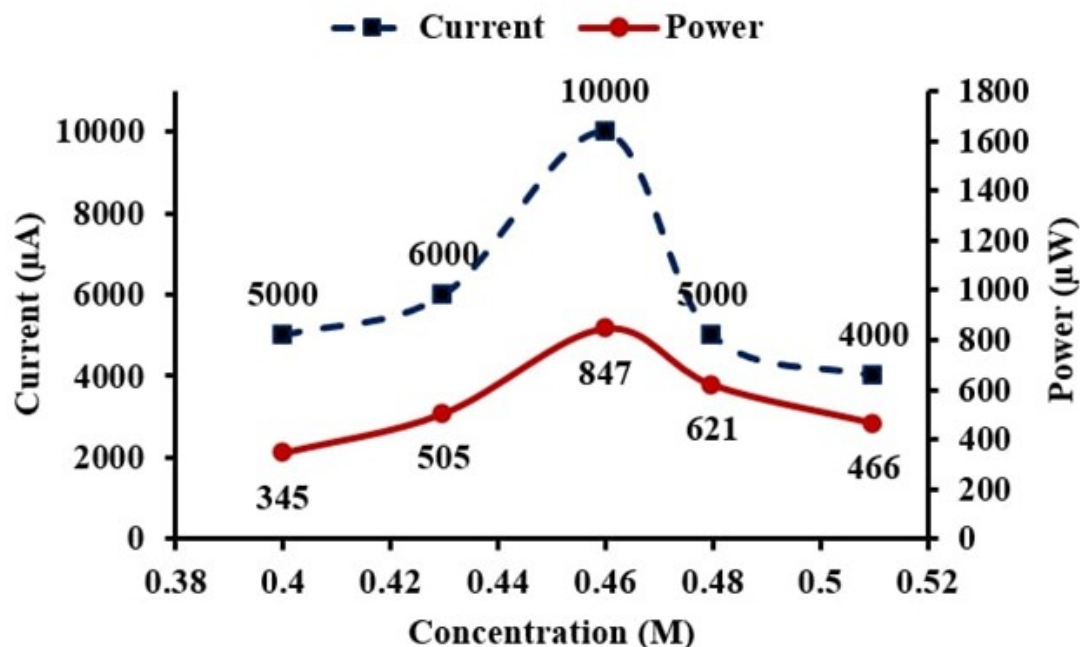


Figure 7: The effect of variation of alkali (sodium hydroxide, NaOH) concentration on the cell performance, (1) Current (i_{\max}) vs Concentration (upper curve); (2) Power at power point (P_{pp}) vs Concentration (lower curve); $^{\#}$ [Cellobiose] 0.29×10^{-3} M, [Neutral Red Dye] 0.30×10^{-4} M, [DTAB] 2.86×10^{-3} M, [NaOH] 0.46 M, Electrode Area $0.2 \text{ cm} \times 0.15 \text{ cm}$, Light Intensity 30 mW cm^{-2} , Diffusion Length 5 cm

Table 6: Chemical composition of the cells fabricated for optimization of the dye concentration

Cell S.N.	Volume of solutions of chemicals used to prepare 35 ml mixture [#]					Resultant concentrations			
	1M NaOH (ml)	M/500 Neutral Red (ml)	M/100 Cellobiose (ml)	M/10 DTAB (ml)	Distilled Water (ml)	NaOH (M)	Neutral Red $\times 10^{-4}$ M	Cellobiose $\times 10^{-3}$ M	DTAB $\times 10^{-3}$ M
1.	16	0.1	1.0	1.0	16.9	0.46	0.06	0.29	2.86
2.	16	0.3	1.0	1.0	16.7	0.46	0.17	0.29	2.86
3.	16	0.5	1.0	1.0	16.5	0.46	0.30	0.29	2.86
4.	16	0.7	1.0	1.0	16.3	0.46	0.40	0.29	2.86
5.	16	0.9	1.0	1.0	16.1	0.46	0.51	0.29	2.86

[#]Pt Electrode Area $0.2 \text{ cm} \times 0.15 \text{ cm}$, cylindrical graphite counter electrode, Light Intensity 30 mW cm^{-2} , Diffusion Length 5 cm

Red, which is a non-ionic dye. Improved solubility leads to better diffusion capabilities for the dye molecules within the electrolyte, which directly translates to enhanced cell performance. Conversely, at lower pH values (lower NaOH concentrations), the dye undergoes protonation, which limits its tendency to donate electrons, resulting in a reduced current

output from the cell. However, beyond the optimized alkali concentration of 0.46 M (corresponding to a pH of 13.45), the electrical parameters of the cell begin to deteriorate. This decline is likely due to an excessive concentration of hydroxide (OH^-) ions, which can interfere with the crucial reductant regeneration cycle, as illustrated in Figure 7. The

cyclic regeneration of the reductant is essential for the continuous operation of photogalvanic cells, as is the regeneration of other species involved in the

electrochemical cycle. The existence of an optimal NaOH concentration, rather than a monotonic increase or decrease, highlights a delicate balance of

Table 7: Electrical parameters of the five different cells fabricated by variation of the Neutral Red dye photosensitizer

Cell Parameters	[Neutral Red] $\times 10^{-4}$ M [#]				
	0.06	0.17	0.30	0.40	0.51
V_{dark} (mV)	488	504	546	500	486
V_{max} (mV)	877	896	916	903	894
V_{OC} (mV)	875	890	910	898	890
Charging time (min.)	16	16	14	14	15
i_{max} (μA)	6000	6500	10000	7000	5000
i_{SC} (μA)	5000	5600	8000	6000	5000
P_{pp} (μW)	396	638	847	575	431
V_{pp}	330	456	603	442	359
i_{pp}	1200	1400	1400	1300	1200
C.E. (%)	3.98	9.09	10.95	6.81	4.63
F.F.	0.09	0.13	0.12	0.11	0.10

[#] [Cellobiose] 0.29×10^{-3} M, [NaOH] 0.46 M, [DTAB] 2.86×10^{-3} M, Electrode Area $0.2 \text{ cm} \times 0.15 \text{ cm}$, Light Intensity 30 mW cm^{-2} , Diffusion Length 5 cm

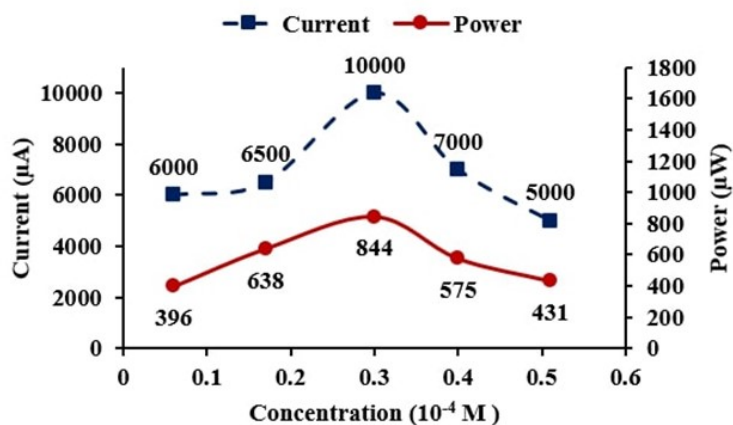


Figure 8: The effect of variation of Neutral Red dye concentration. (1) Current (i_{max}) vs Concentration (upper curve); (2) Power at power point (P_{pp}) vs Concentration (lower curve); [#][Cellobiose] 0.29×10^{-3} M, [NaOH] 0.46 M, [DTAB] 2.86×10^{-3} M, Electrode Area $0.2 \text{ cm} \times 0.15 \text{ cm}$, Light Intensity 30 mW cm^{-2} , Diffusion Length 5 cm

competing effects. While increased alkalinity aids dye solubility and diffusion, excessive OH^- ions hinder reductant regeneration, underscoring the importance of precise pH control in photogalvanic systems.

Previous research has established that an alkalinity range of pH 12 to 14 is most suitable for maximizing dye solubility and promoting favorable electrochemical properties of sensitizer molecules for solar power generation. Figure 7 clearly illustrates

Table 8: Chemical composition of cells produced for the Dodecyltrimethyl Ammonium Bromide concentration optimization

Cell S.N.	Volume of solutions of chemicals used to prepare 35 ml electrolyte mixture					Resultant concentrations			
	1M NaOH (ml)	M/500 Neutral Red (ml)	M/100 Cellobiose (ml)	M/10 DTAB (ml)	Distilled Water (ml)	NaOH M	Neutral Red $\times 10^{-4}$ M	Cellobiose $\times 10^{-3}$ M	DTAB $\times 10^{-3}$ M
1.	16	0.5	1.0	0.1	17.4	0.46	0.30	0.29	0.29
2.	16	0.5	1.0	0.5	17.0	0.46	0.30	0.29	1.43
3.	16	0.5	1.0	1.0	16.5	0.46	0.30	0.29	2.86
4.	16	0.5	1.0	1.5	16.0	0.46	0.30	0.29	4.29
5.	16	0.5	1.0	2.0	16.5	0.46	0.30	0.29	5.71

[#]Pt Electrode Area $0.2 \text{ cm} \times 0.15 \text{ cm}$, cylindrical graphite counter electrode, Light Intensity 30 mW cm^{-2} , Diffusion Length 5 cm

Table 9: The effect of variation of concentration of Dodecyltrimethyl Ammonium Bromide (DTAB) as surfactant on cell performance

Cell Parameters	[DTAB] $\times 10^{-3} \text{ M}^{\#}$				
	0.29	1.43	2.86	4.29	5.71
V_{dark} (mV)	499	510	546	513	504
V_{max} (mV)	898	901	916	895	879
V_{OC} (mV)	894	897	910	889	875
Charging time (min.)	17	16	14	15	15
i_{max} (μA)	7000	8000	10000	8000	6000
i_{SC} (μA)	5000	6000	8000	7000	6500
P_{PP} (μW)	522	685	847	637	534
V_{PP}	435	489	605	490	445
i_{PP}	1200	1400	1400	1300	1200
C.E. (%)	6.77	9.68	10.95	7.24	5.57
F.F.	0.12	0.13	0.12	0.10	0.09

[#] At [Cellobiose] $0.29 \times 10^{-3} \text{ M}$, [NaOH] 0.46 M , [Neutral Red Dye] $0.30 \times 10^{-4} \text{ M}$, Electrode Area $0.2 \text{ cm} \times 0.15 \text{ cm}$, Light Intensity 30 mW cm^{-2} , Diffusion Length 5 cm

the relationship between NaOH concentration and the cell's maximum current (i_{max}) and power at power point (P_{PP}). The curves show an initial increase in both parameters, reaching a peak at 0.46 M NaOH, followed by a decline at higher concentrations. This visual representation reinforces the quantitative data from the tables, making the optimal concentration and the trend of performance change with alkali concentration immediately clear.

4.2 Impact of Neutral Red Dye Photosensitizer Concentration

The concentration of the Neutral Red dye photosensitizer is another pivotal factor governing the photogalvanic cell's performance. To systematically evaluate its influence, five distinct cells were fabricated, each containing a different concentration of Neutral Red dye, while ensuring that

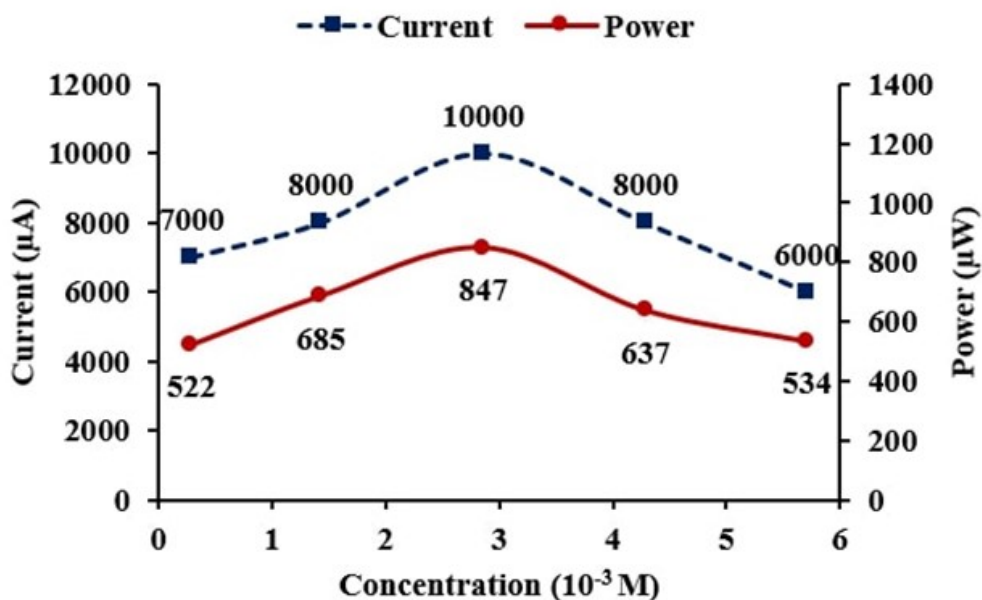


Figure 9: Variation of DTAB surfactant concentration#, (1) Current (i_{\max}) vs Concentration (upper curve); (2) Power at power point (P_{pp}) vs Concentration (lower curve); #At [Cellobiose] 0.29×10^{-3} M, [NaOH] 0.46 M, [Neutral Red Dye] 0.30×10^{-4} M, Electrode Area $0.2 \text{ cm} \times 0.15 \text{ cm}$, Light Intensity 30 mW cm^{-2} , Diffusion Length = 5 cm

Table 10: Chemical composition of the cells fabricated for optimization of the reductant concentration

Cell S.N.	Volume of solutions of chemicals used to prepare 35 ml mixture [#]					Resultant concentrations			
	1M NaOH (ml)	M/500 Neutral Red (ml)	M/100 Cellobiose (ml)	M/10 DTAB (ml)	Distilled Water (ml)	NaOH M	Neutral Red $\times 10^{-4}$ M	Cellobiose $\times 10^{-3}$ M	DTAB $\times 10^{-3}$ M
1.	16	0.5	0.1	1.0	17.4	0.46	0.30	0.03	2.86
2.	16	0.5	0.5	1.0	17.0	0.46	0.30	0.14	2.86
3.	16	0.5	1.0	1.0	16.5	0.46	0.30	0.29	2.86
4.	16	0.5	1.3	1.0	16.2	0.46	0.30	0.37	2.86
5.	16	0.5	1.5	1.0	16.0	0.46	0.30	0.43	2.86

[#]Pt Electrode Area $0.2 \text{ cm} \times 0.15 \text{ cm}$, cylindrical graphite counter electrode, Light Intensity 30 mW cm^{-2} , Diffusion Length 5 cm.

concentrations of other chemical components (NaOH alkali, Cellobiose reductant, and DTAB surfactant) and physical parameters (diffusion length, electrode area, and light intensity) remained constant. The chemical compositions of these cells are provided in Table 6, and their electrical parameters are detailed in Table 7.

The electrical parameters of the cell varied significantly with different concentrations of Neutral Red dye photosensitizer. As the dye photosensitizer concentration was incrementally increased, a corresponding rise in the cell's power output was observed, reaching a distinct maximum value. Beyond this peak, further increases in dye

concentration led to a decline in power output. The optimum electrical output was specifically obtained at a dye concentration of 0.30×10^{-4} M, which

Table 11: Electrical parameters of the five different cells fabricated by the variation of the Cellobiose concentration

Cell Parameters	[Cellobiose] $\times 10^{-3}$ M [#]				
	0.03	0.14	0.29	0.37	0.43
V_{dark} (mV)	489	501	546	490	487
V_{max} (mV)	902	908	916	896	892
V_{OC} (mV)	897	904	910	890	888
t_{charging} (min.)	16	16	14	15	15
i_{max} (μA)	6000	8000	10000	9000	8000
i_{SC} (μA)	5500	7000	8000	6500	6000
P_{pp} (μW)	490	701	847	645	602
V_{PP}	490	501	605	496	430
i_{PP}	1000	1400	1400	1300	1400
C.E. (%)	5.41	8.64	10.95	7.99	7.56
F.F.	0.10	0.11	0.12	0.11	0.11

[#] At [DTAB] 2.86×10^{-3} M, [NaOH] 0.46 M, [Neutral Red Dye] 0.30×10^{-4} M, Electrode Area $0.2 \text{ cm} \times 0.15 \text{ cm}$, Light Intensity 30 mW cm^{-2} , Diffusion Length 5 cm

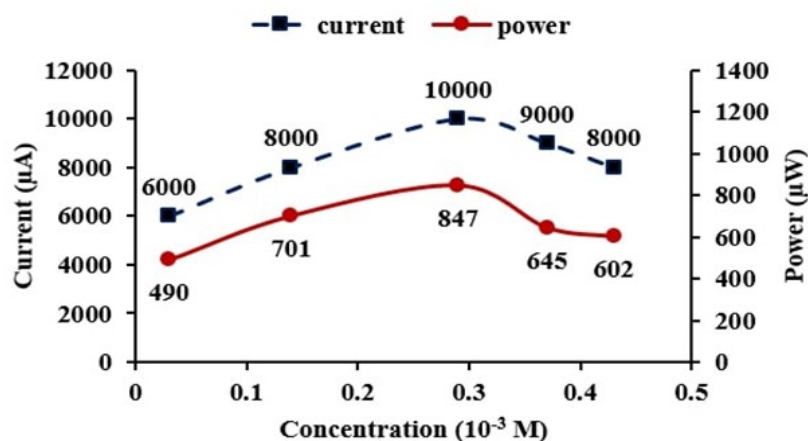


Figure 10: Variation of cellobiose reductant concentration (1) Current (i_{max}) vs Concentration (upper curve); (2) Power at power point (P_{pp}) vs Concentration (lower curve) [#]At [DTAB] 2.86×10^{-3} M, [NaOH]0.46 M, [Neutral Red Dye] 0.30×10^{-4} M, Electrode Area $0.2 \text{ cm} \times 0.15 \text{ cm}$, Light Intensity 30 mW cm^{-2} , Diffusion Length 5 cm

However, exceeding this optimum dye concentration introduces detrimental effects. At excessively high concentrations, the dye molecules tend to aggregate. This aggregation significantly hinders the efficient

diffusion of dye molecules towards the platinum electrode, which is crucial for continuous electrochemical reactions, leading to a reduction in both current and power. Furthermore, an

Table 12: Variation of platinum electrode size (five different cells fabricated with different sizes of platinum electrodes)

Electrical parameters	Size of the Platinum Electrode [#]				
	0.03 cm ² (0.2 × 0.15)	0.25 cm ² (0.5 × 0.5)	0.7 cm ² (1 × 0.7)	1.0 cm ² (1 × 1)	1.5 cm ² (1 × 1.5)
i_{\max} (μA)	10000	8000	6500	5000	3500
i_{SC} (μA)	8000	6000	5000	3500	3000
V_{OC} (mV)	910	890	840	855	820
P_{PP} (μW)	847	639	461	372	336
V_{PP}	605	456	355	310	280
i_{PP}	1400	1400	1300	1200	1200
C.E. (%)	10.95	1.02	0.24	0.15	0.10
F.F.	0.12	0.12	0.11	0.12	0.14

[#] At [DTAB] 2.86×10^{-3} M, [NaOH]0.46 M, [Neutral Red Dye] 0.30×10^{-3} M, Electrode Area 0.2 cm × 0.15 cm, Light Intensity 30 mW cm⁻², Diffusion Length 5 cm

Table 13: Variation of illuminating intensity (five identical cells with optimum concentration of dye, reductant, surfactant, and alkali)

Electrical Parameters	Illuminating Intensity (mW cm ⁻²) [#]				
	12	15	18	30	38
i_{\max} (μA)	8000	9000	9000	10000	8000
i_{SC} (μA)	7800	7900	8000	8000	7900
V_{OC} (mV)	900	900	905	910	890
P_{PP} (μW)	500	586	650	847	840
V_{PP}	500	533	542	605	600
i_{PP}	1000	1100	1200	1400	1400
t_{Charging} (min.)	16	16	16	14	12
C.E. (%)	9.89	10.74	10.82	10.95	8.80
F.F.	0.07	0.08	0.09	0.12	0.12

[#] At [Cellobiose] 0.29×10^{-3} M, [DTAB] 2.86×10^{-3} M, [NaOH]0.46 M, [Neutral Red Dye] 0.30×10^{-3} M, Electrode Area 0.2 cm × 0.15 cm, Light Intensity 30 mW cm⁻², Diffusion Length 5 cm

exceptionally large number of dye molecules at concentrations greater than the optimum can also impede performance by (i) preventing photons from effectively reaching the ground state dye species located near the platinum electrode, and (ii) obstructing the movement of excited state dye species or semi/leuco-reduced dye species from reaching the electrode surface.¹ This cumulative

effect results in a decrement in the overall cell performance. The phenomenon of performance decreasing beyond an optimal dye concentration is a critical observation, indicating limitations due to self-quenching or aggregation effects commonly encountered in dye-sensitized systems. This implies that simply increasing the amount of photosensitizer is counterproductive and underscores the importance

Table 14: Variation of illuminating window size (five different cells fabricated with optimum concentration of dye, reductant, surfactant, and alkali)

Electrical Parameters	Size of The Illumination Window (cm × cm)			
	0.5 × 0.5	1 × 1	1 × 2	1 × 3
i_{\max} (μA)	7500	8000	7000	7000
i_{SC} (μA)	6500	8000	7000	6800
V_{OC} (mV)	908	910	901	900
P_{PP} (μW)	718	847	763	747
V_{PP}	598	605	587	575
i_{PP}	1200	1400	1300	1300
t_{Charging} (min.)	16	14	12	12
C.E. (%)	9.69	10.95	10.26	10.14
F.F.	0.12	0.12	0.12	0.12

[#]At [Cellobiose] 0.29×10^{-3} M, [DTAB] 2.86×10^{-3} M, [NaOH] 0.46 M, [Neutral Red Dye] 0.30×10^{-3} M, Electrode Area $0.2 \text{ cm} \times 0.15 \text{ cm}$, Light Intensity 30 mW cm^{-2} , Diffusion Length 5 cm

of balancing light absorption with efficient charge transport.

Figure 8 graphically illustrates the relationship between Neutral Red dye concentration and the cell's maximum current (i_{\max}) and power at power point (P_{PP}). The curves clearly show an initial increase in performance with increasing dye concentration, reaching a distinct peak, and then a subsequent decline at higher concentrations. This "bell-shaped" curve is characteristic of many chemical reactions where an optimal concentration exists, and in this context, it visually confirms the detrimental effects of dye aggregation and light screening at supra-optimal concentrations.

4.3 Effect of Dodecyl trimethyl Ammonium Bromide (DTAB) Surfactant Concentration

The concentration of Dodecyl trimethyl Ammonium Bromide (DTAB) surfactant was systematically investigated for its impact on the photogalvanic cell's performance. Five cells were prepared with varying DTAB concentrations, while maintaining constant concentrations of the Neutral Red dye photosensitizer, NaOH alkali, and Cellobiose reductant. Other cell fabrication parameters, including diffusion length, electrode area, and light intensity, were also kept constant across all these experimental setups. The chemical compositions used for this optimization are listed in Table 8, and the resulting electrical performance data is presented in Table 9.

The electrical performance of the photogalvanic cells, as a function of DTAB concentration, followed a distinct trend. Initially, as the concentration of DTAB increased, the cell's performance improved, reaching an optimum value at 2.86×10^{-3} M DTAB. However, at DTAB concentrations exceeding this optimal point, a decline in the electrical performance of the cell was observed.

This behavior can be attributed to the surfactant's ability to influence the solubility and diffusion characteristics of the dye within the electrolyte solution. DTAB, being a cationic surfactant, enhances the solubility and dispersibility of the Neutral Red dye, which in turn facilitates its transport and reactivity, thereby improving the electrical performance of the cell as its concentration increases. This effect is particularly pronounced as the surfactant concentration approaches and surpasses its critical micelle concentration (CMC), where micelles form and aid in solubilization.

However, exceeding the optimal DTAB concentration leads to a reduction in cell performance. This decline is likely due to an excessive number of surfactant molecules, which can hinder the crucial diffusion process of the active species within the electrolyte. Previous studies have reported that while dye solubilization increases once the surfactant reaches its CMC, further increases in surfactant concentration beyond a certain point may not significantly impact dye solubility. Moreover, at very high surfactant concentrations, the formation of

Table 15: Comparative analysis of recent photogalvanic (PG) cells with the present Neutral Red–DTAB–cellobiose system

#	Study (Year, Publisher / Journal)	Photosensitizer (Dye)	Reductant	Surfactant / Medium	Photo-potential (mV)	Photo-current (μA)	Efficiency / Power
1	Present study	Neutral Red	Cellobiose	DTAB (non-ionic surfactant)	916	10 000	10.95 % (847 μW)
2	Bhimwal & Gangotri, Energy, 2011 (Elsevier) (K. M. Gangotri & Bhimwal, 2011)	Rose Bengal / Toluidine Blue	D-Xylose	NaLS micellar	802	320	0.07–0.10 %
3	Genwa et al., Material Science, 2015 (De Gruyter) (Genwa & Shraddha, 2015)	Phloxin B	EDTA	CTAB	1135	300	0.64 %
4	Koli et al., Applied Energy, 2014 (Elsevier) (Koli, 2014b)	Fast Green FCF	Fructose	Alkaline medium (NaOH)	1083	431	1.33 % (138.6 μW)
5	Gangotri and Gangotri et, Energy Sources, 2013 (T&F) (P. Gangotri & Gangotri, 2013)	Safranin O	EDTA	Sodium Lauryl Sulphate	871	200	0.7213 % (75.02 μW)
6	Yadav and Lal, Energy Conversion and Management journal, 2023 (Elsevier) (Yadav & Lal, 2013)	Brilliant Green + Celestine Blue)	EDTA	NA	93	636	0.31 % (59.1 μW)

rod-like micelles can occur, leading to a considerable increase in solution viscosity. This elevated viscosity negatively impacts the diffusion of dye molecules and other reactive species, consequently reducing the cell's electrical performance. The optimal DTAB concentration and the subsequent performance drop due to excessive surfactant hindering diffusion directly relate to the concepts of Critical Micelle Concentration (CMC) and micellar structure changes. This indicates that DTAB's role extends beyond simply increasing solubility; it also involves maintaining optimal solution viscosity and micellar morphology for efficient transport of active species.

Figure 9 graphically illustrates the relationship between DTAB surfactant concentration and the cell's maximum current (i_{max}) and power at power point (P_{pp}). The graph clearly shows an increase in

performance up to an optimal DTAB concentration of 2.86×10^{-3} M, followed by a decrease at higher concentrations. This visual representation supports the quantitative data, confirming the optimal surfactant concentration and the subsequent performance drop, which is characteristic of surfactant behavior influenced by micelle formation and solution viscosity.

4.4 Role of Cellobiose Reductant Concentration

The concentration of cellobiose, serving as the reductant, was another critical parameter subjected to systematic optimization. To investigate its effect on cell performance, five cells were fabricated, each containing a different concentration of cellobiose,

while maintaining constant concentrations of Neutral Red dye photosensitizer, NaOH alkali, and DTAB surfactant. All other cell fabrication parameters, including diffusion length, electrode area, and light intensity, were also kept constant. The chemical compositions for these experiments are provided in Table 10, and the resulting electrical performance data is presented in Table 11.

The electrical performance of the photogalvanic cells demonstrated a clear dependence on the concentration of Cellobiose. As the Cellobiose concentration was increased, the cell's performance improved, reaching an optimal value at 0.29×10^{-3} M. Beyond this optimal concentration, decreased electrical performance of the cell was observed. The electrical performance of the photogalvanic cells demonstrated a clear dependence on the concentration of Cellobiose. As the Cellobiose concentration was increased, the cell's performance improved, reaching an optimal value at 0.29×10^{-3} M. Beyond this optimal concentration, decreased electrical performance of the cell was observed.

The initial improvement in cell performance with increasing Cellobiose concentration is directly attributable to the increased availability of reductant molecules. A higher concentration of Cellobiose ensures that more reductant molecules are readily available to reduce the excited dye molecules, thereby facilitating efficient electron transfer and sustained photocurrent generation.

However, when the concentration of the reductant is increased beyond its optimal value (i.e., 0.29×10^{-3} M), the system's performance deteriorates. This decline is likely due to an excessive number of reductant molecules interfering with the critical diffusion process within the cell. In electrochemical systems, while reactants are necessary, their over-concentration can impede mass transport, which is crucial for continuous operation. This suggests a delicate balance between reaction kinetics, which benefit from higher reactant concentrations, and diffusion rates, which can be hindered by excessive molecular crowding. Therefore, achieving an optimal reductant concentration is essential for maximizing the cell's electrical performance without compromising the efficient transport of species.

Figure 10 graphically illustrates the relationship between cellobiose reductant concentration and the cell's maximum current (i_{max}) and power at power point (P_{pp}). The graph shows an initial increase in performance, peaking at 0.29×10^{-3} M Cellobiose, followed by a decrease at higher concentrations. This visual representation confirms the optimal reductant

concentration and the subsequent performance drop, similar to other concentration-dependent effects where an excess of a component can become detrimental.

4.5 Optimization of Platinum Electrode Size

The size of the platinum electrode, serving as the working electrode, is a critical physical parameter that significantly influences the electrical performance of the photogalvanic cell. To optimize this parameter, five cells were fabricated, each incorporating a platinum electrode of a different size, while maintaining constant concentrations of all chemical components (Neutral Red dye photosensitizer, NaOH alkali, Cellobiose reductant, and DTAB surfactant) and other physical parameters such as diffusion length, counter electrode type, and light intensity. The electrical performance data for these varying platinum electrode sizes are presented in Table 12.

The electrical data revealed that the optimum performance of the cell was achieved with a platinum electrode area of 0.03 cm^2 for the investigated system. A notable observation was that as the size of the platinum electrode increased beyond this optimal area, the performance of the cell progressively declined. This counter-intuitive finding, where a smaller electrode area leads to optimal performance, strongly suggests that the rate-limiting step in this photogalvanic system is not solely the electron transfer at the electrode surface area, but rather the efficient *diffusion* of electroactive ions to and from the electrode surface. Photogalvanic cells are highly dependent on the phenomenon of ion diffusion, and a smaller electrode area appears to facilitate the ease of ion diffusion within the electrolyte solution. This implies that maximizing surface area is less critical than ensuring efficient mass transport in this specific system.

Platinum was chosen as the electrode material due to its extensive use in previous photogalvanic cell studies. Beyond its established utility, platinum is a noble metal, offering high resistance to corrosion, and possessing excellent electrical and mechanical properties. From an economic perspective, platinum is an expensive material. Therefore, minimizing the size of the electrodes, as indicated by the optimization results, contributes to making the fabrication of the photogalvanic cell more cost-effective without compromising performance.

4.6 Effect of Illumination Intensity

The influence of light intensity on the photogalvanic cell's performance was investigated by systematically varying the distance between the platinum electrode

and the light source, a 200-watt incandescent bulb. The corresponding light intensity at each distance was measured using a Solar Meter. Five identical cells, each prepared with the optimized concentrations (1 ml of M/100 Cellobiose, 16 ml of 1M NaOH, 0.5 ml of M/500 Neutral Red dye, and 1 ml of M/10 DTAB), were used for this study. The results obtained from this investigation are summarized in Table 13.

The results indicate that the variation in the electrical performance of the cell with changes in illuminating intensity was remarkably small. A slight increase in cell performance was observed as the distance from the light source decreased (corresponding to increasing intensity), up to a certain proximity of illumination. This initial improvement is attributable to the increased number of photons available for the excitation of the dye sensitizer molecules.

However, beyond this optimal illumination intensity, the heating effect generated by the 200-watt incandescent bulb, used as the light source in this study, began to cause a deterioration in the cell's performance. The observation of minimal variation in performance with light intensity, and even deterioration at very high intensities due to heating, is a significant finding. This suggests that the cell is not highly sensitive to light intensity fluctuations within a certain range, which could be an advantage for real-world applications where ambient light conditions can vary. It also highlights the critical importance of thermal management in the design of efficient photogalvanic cells, particularly when operating under high illumination or with light sources that generate considerable heat.

4.7 Influence of Illumination Window Size

The effect of varying the size of the illumination window on the cell's performance was also investigated. Four cells were fabricated, each with the optimized concentrations of Cellobiose (1 ml of M/100), NaOH (16 ml of 1M), Neutral Red dye (0.5 ml of M/500), and DTAB surfactant (1 ml of M/10), but with different illumination window sizes as tabulated in Table 14.

The study revealed that there was no significant effect of the variation in window size on the electrical performance of the cell. This observation can be understood by considering the inherent properties of the constructed cell and the nature of light. Each fabricated cell contained a specific molar concentration of dye molecules, which, according to Avogadro's number, corresponds to a definite number of dye molecules. For these dye molecules to

undergo photoexcitation, a specified number of photons is required.

Crucially, the light intensity per unit area entering through the illumination window remained constant across all scenarios, regardless of the window's size. Consequently, when the illumination window was at its smallest (0.5 cm×0.5 cm), the total number of photons entering the electrolyte per unit time was at its lowest. As a direct result, the cell required a comparatively longer illumination time (20 minutes) for its charging process to ensure an adequate number of photons were available for the photoexcitation of the requisite number of sensitizer molecules. This longest charging time was indeed noted for the smallest illumination window size in the current study. Conversely, as the illumination window size increased, the total quantity of photons entering the electrolyte per unit time increased proportionally, leading to a reduction in the required charging time. This finding is consistent with previous studies, which have demonstrated that photogalvanic cells can operate effectively even at low illumination intensities. The lack of significant influence of illumination window size on the overall electrical performance can be attributed to the properties of light waves, specifically diffraction and scattering, within the H-shaped photogalvanic cell. These phenomena ensure that the complete volume of the electrolyte solution is effectively illuminated, regardless of the precise window dimensions. The lack of significant effect of illumination window size on electrical performance, despite affecting charging time, is a crucial distinction. This implies that the total energy input (photon quantity) primarily dictates the charging rate, but the overall efficiency is more robust against variations in the illuminated area due to light diffusion and scattering within the H-shaped cell, suggesting flexibility in cell design regarding light collection.

Based on a thorough analysis of the optimization experiment data, the ideal fabrication variables for this photogalvanic system have been precisely established. The optimal concentrations for the system components are as follows: cellobiose at 0.29×10^{-3} M, DTAB at 2.86×10^{-3} M, NaOH at 0.40 M, and Neutral Red dye at 0.30×10^{-4} M. The platinum electrode used in the cell has an area of 0.2 cm × 0.15 cm, and the diffusion length is maintained at 5 cm. Illumination intensity is set at 30 mW/cm², ensuring consistent photoexcitation across the cell. Under these optimized conditions, the photogalvanic system demonstrates impressive electrical performance. It achieves a maximum potential and photopotential of 916 mV, while the

maximum current reaches 10,000 μA and the short circuit current is 8,000 μA . The power at the power point is measured at 847 μW , with a fill factor of 0.26 and a conversion efficiency of 10.95%.

The Neutral Red–DTAB–cellobiose system demonstrates a photocurrent of 10,000 μA and efficiency of 10.95 %, representing a great improvement over the best previously reported systems. While the photopotential (916 mV) is comparable to earlier results, the exceptionally high current density drives the substantial gain in efficiency. The synergistic interaction of the DTAB surfactant with the cellobiose reductant in an alkaline medium enhances charge-transfer kinetics and overall conversion stability.

5. CONCLUSION

This study thoroughly investigated the photogalvanic properties of a system comprising Neutral Red dye photosensitizer, DTAB surfactant, cellobiose reductant, and Sodium Hydroxide alkali in an aqueous medium, with a focus on solar energy conversion and storage. The research successfully demonstrated a substantial improvement in the electrical performance of photogalvanic cells when compared to previous studies.

The optimized system achieved a maximum potential of 916 mV, a maximum current of 10000 μA , and a power at power point of 847 μW . Furthermore, it exhibited a fill factor of 0.26 and a conversion efficiency of 10.95%. This enhanced photogalvanic performance is attributed to a synergistic combination of carefully optimized factors related to both the electrode properties and the chemical composition of the cell. These include maintaining a high pH, the utilization of cellobiose as a reducing sugar, the inherent properties of the non-ionic Neutral Red dye, the presence of cationic DTAB surfactant, and the strategic use of a small-sized platinum electrode.

The high alkalinity of the medium, the presence of DTAB surfactant, and the selection of a small-sized platinum electrode collectively contribute to enhanced solubility, photo-stability, and diffusivity of the sensitizer molecules within the electrolyte. Specifically, the reduction in the size of the platinum electrode was found to significantly facilitate better ionic diffusion, which is a critical factor for efficient photogalvanic operation. These combined and optimized factors ultimately led to the observed high electrical parameters of the cell. The success of this study underscores that the improved performance is not due to any single factor in isolation, but rather a complex and interconnected interplay of optimized

parameters, reinforcing the importance of a holistic approach to photogalvanic cell design.

Acknowledgement

The authors gratefully acknowledge the Department of Chemistry, Jai Narain Vyas University, Jodhpur, Rajasthan, India, for providing essential laboratory facilities and a supportive environment for this research. Authors are also thankful to the DRDO Lab, Jodhpur, Government of India, for access to their spectroscopic facilities.

Conflict of Interest

The author has no conflict of interest to declare.

Data Availability Statement

All the experimental data has already been incorporated into the manuscript and supporting information.

Funding

This research did not receive any specific grant from funding agencies in the public, commercial, or not-for-profit sectors.

REFERENCES

- Albery, W. J. (1982). Development of Photogalvanic Cells for Solar Energy Conversion. *Accounts of Chemical Research*, 15(5), 142–148. <https://doi.org/10.1021/ar00077a003>
- Ameta, S. C., Dubey, G. C., Dubey, T. D., & Ameta, R. (1985). Studies in the photochemical conversion of solar energy II. Use of toluidine blue-nitriloacetic acid in a photogalvanic cell. *Z. Phys. Chem.*, 266(1), 200–203. <https://doi.org/10.1515/zpch-1985-26631>
- Bahri, M. A., Hoebeke, M., Grammenos, A., Delanaye, L., Vandewalle, N., & Seret, A. (2006). Investigation of SDS, DTAB and CTAB micelle microviscosities by electron spin resonance. *Colloids and Surfaces A: Physicochemical and Engineering Aspects*, 290(1–3), 206–212. <https://doi.org/10.1016/j.colsurfa.2006.05.021>
- Becquerel, K. (1839). Memoire sur les effets electriques produits sous l'influence des rayons solaires.
- Gangotri, K. M., & Bhimwal, M. K. (2011). A study of the performance of the photogalvanic cells for solar energy conversion and storage: Methyl orange-D-xylose-NaLS system. *Energy Sources, Part A: Recovery, Utilization, and Environmental Effects*, 33(22), 2058–2066. <https://doi.org/10.1080/15567030903503209>

- Gangotri, K. M., & Lal, C. (2000). Studies in photogalvanic effect and mixed dyes system: EDTA-methylene blue + toluidine blue system. *International Journal of Energy Research*, 24(4), 365–371. [https://doi.org/10.1002/\(SICI\)1099-114X\(20000325\)24:4<365::AID-ER593>3.0.CO;2-I](https://doi.org/10.1002/(SICI)1099-114X(20000325)24:4<365::AID-ER593>3.0.CO;2-I)
- Gangotri, K. M., & Regar, O. P. (1996). Role of azine dye as photosensitizer in solar cell: Glucose-safranine system. *Heterocycl. Commun.*, 2(6), 567–572. <https://doi.org/10.1515/hc.1996.2.6.567>
- Gangotri, P., & Gangotri, K. M. (2013). Studies of the micellar effect on photogalvanics: Solar energy conversion and storage - EDTA-safranine O-NaLS system. *Energy Sources, Part A: Recovery, Utilization and Environmental Effects*, 35(11), 1007–1016. <https://doi.org/10.1080/15567030903077980>
- Genwa, K. R., & Shraddha. (2015). Photocurrent response of phloxin B-cetyltrimethylammonium bromide photogalvanic cell device. *Materials Science- Poland*, 33(3), 612–619. <https://doi.org/10.1515/msp-2015-0090>
- Green, M. A., Dunlop, E. D., Hohl-Ebinger, J., Yoshita, M., Kopidakis, N., Bothe, K., Hinken, D., Rauer, M., & Hao, X. (2022). Solar cell efficiency tables (Version 60). *Progress in Photovoltaics: Research and Applications*, 30(7), 687–701. <https://doi.org/10.1002/pip.3595>
- Hillson, P. J., & Rideal, E. (1953). The Becquerel effect in the presence of dyestuffs and the action of light on dyes.
- Hoffman, M. Z., & Lichtin, N. N. (1979). Photochemical Determinants of the Efficiency of Photogalvanic Conversion of Solar Energy. In: R. R. Hautala, R. B. King, & C. Kutal (eds) *Solar Energy. Contemporary Issues in Science and Society*; pp. 153–187. Humana Press. https://doi.org/10.1007/978-1-4612-6245-9_7
- IEA (2020). *Evolution of solar PV module cost by data source, 1970-2020*, IEA, Paris. Retrieved August 29, 2025, from <https://www.iea.org/data-and-statistics/charts/evolution-of-solar-pv-module-cost-by-data-source-1970-2020>
- Jonwal, M., Koli, P., Dayma, Y., Kumar Pareek, R., Kumar, R., & Dheerata. (2022). Photogalvanics of Dodecyltrimethyl Ammonium Bromide-Quinoline Yellow-alkali: A solar energy conversion, storage, photostability, and spectral study. *International Journal of Energy Research*, 46(10), 13889–13907. <https://doi.org/10.1002/er.8106>
- Jonwal, M., Koli, P., & Kumar, R. (2025). Natural surfactant fenugreek (*Trigonella foenum-graecum*) seeds based photogalvanic cell for solar energy conversion and storage. *Results in Chemistry*, 15(March), 102220. <https://doi.org/10.1016/j.rechem.2025.102220>
- Kaneko, M., & Yamada, A. (1977). Photopotential and photocurrent induced by a tolusafranine-ethylenediaminetetraacetic acid system [1]. *Journal of Physical Chemistry*, 81(12), 1213–1215. <https://doi.org/10.1021/j100527a020>
- Koli, P. (2014a). Photogalvanic cells: Comparative study of various synthetic dyes and natural photo sensitizers present in spinach extract. *RSC Advances*, 4(86), 46194–46202. <https://doi.org/10.1039/c4ra08373c>
- Koli, P. (2014b). Solar energy conversion and storage: Fast Green FCF-Fructose photogalvanic cell. *Applied Energy*, 118, 231–237. <https://doi.org/10.1016/j.apenergy.2013.12.035>
- Koli, P., & Saren, J. (2024). Photogalvanics of copper and brass working electrodes in the NaOH-Allura Red-d-galactose-DDAC electrolyte for solar power generation. *RSC Advances*, 14(21), 14648–14664. <https://doi.org/10.1039/d4ra01091d>
- Koli, P., Sharma, U., & Gangotri, K. M. (2012). Solar energy conversion and storage: Rhodamine B - Fructose photogalvanic cell. *Renewable Energy*, 37(1), 250–258. <https://doi.org/10.1016/j.renene.2011.06.022>
- Lal, C. (2007). Use of mixed dyes in a photogalvanic cell for solar energy conversion and storage: EDTA-thionine-azur-B system. *Journal of Power Sources*, 164(2), 926–930. <https://doi.org/10.1016/j.jpowsour.2006.11.020>
- Lal, M., & Gangotri, K. (2025). Comparative study on sunlight induced surfactants system in photogalvanics for solar energy conversion and storage. *Next Sustainability*, 6(August 2024), 100101. <https://doi.org/10.1016/j.nxsust.2025.100101>
- Mall, C., Tiwari, S., & Solanki, P. P. (2022). Evaluation of most efficient redox couple based on compatibility of donor-acceptor in photogalvanic cell for simultaneous solar power conversion and storage. *Journal of Electroanalytical Chemistry*, 926(September), 116950. <https://doi.org/10.1016/j.jelechem.2022.116950>

- Murthy, A. S. N., & Reddy, K. S. (1979). Photochemical Energy Conversion Studies in systems containing methylene blue. *International Journal of Energy Research*, 3(November 1978), 205–210. <https://doi.org/10.1002/er.4440030302>
- NREL. (n.d.). *Photovoltaics-Best Research-Cell Efficiency Chart*. Retrieved August 29, 2025, from <https://www.nrel.gov/pv/cell-efficiency>
- Rabinowitch, E. (1940a). The photogalvanic effect I. The photochemical properties of the thionine-iron system. *The Journal of Chemical Physics*, 8(7), 551–559. <https://doi.org/10.1063/1.1750711>
- Rabinowitch, E. (1940b). The photogalvanic effect II. The photogalvanic properties of the thionine-iron system. *The Journal of Chemical Physics*, 8(7), 560–566. <https://doi.org/10.1063/1.1750712>
- Solanki, P. P., & Gangotri, K. M. (2011). Photogalvanic cell for conversion of solar energy into electricity: Safranine-Arabinose-Sodium lauryl sulphate system. *Solar Energy*, 85(11), 3028–3035. <https://doi.org/10.1016/j.solener.2011.08.043>
- Yadav, S., & Lal, C. (2013). Optimization of performance characteristics of a mixed dye based photogalvanic cell for efficient solar energy conversion and storage. *Energy Conversion and Management*, 66, 271–276. <https://doi.org/10.1016/j.enconman.2012.09.011>
- Zakeri, B., & Syri, S. (2015). Electrical energy storage systems: A comparative life cycle cost analysis. *Renewable and Sustainable Energy Reviews*, 42, 569–596. <https://doi.org/https://doi.org/10.1016/j.rser.2014.10.011>